Journal of Geoscience and Environment Protection, 2025, 13(7), 209-229
https://www.scirp.org/journal/gep
ISSN Online: 2327-4344
ISSN Print: 2327-4336

Mapping the Hydraulic Potential of Fissured Aquifers in the Poni Watershed in South-West Burkina Faso

Hebie Adama, Kafando Sayoba, Nakolendousse Samuel

Geoscience and Environnemental Laboratory (LaGE), Department of Earth Sciences, University of Joseph KI-ZERBO, Ouagadougou, Burkina Faso
Email: altesseroi1@yahoo.fr

How to cite this paper: Adama, H., Sayoba, K., & Samuel, N. (2025). Mapping the Hydraulic Potential of Fissured Aquifers in the Poni Watershed in South-West Burkina Faso. Journal of Geoscience and Environment *Protection, 13,* 209-229.
https://doi.org/10.4236/gep.2025.137013

Received: May 30, 2025
Accepted: July 21, 2025
Published: July 24, 2025

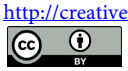

Abstract

The Poni watershed, located in southwest Burkina Faso, is characterized by crystalline basement geological formations. The hydrogeology of the watershed is characterized by two types of aquifers: alterite aquifers and fissured aquifers. Fissured aquifers are still the most widely used for drinking water supply. The general objective of the present work is to map the hydraulic potential of fissured aquifers in the Poni watershed, in order to identify areas with high hydraulic potential for sustainable and rational management of groundwater resources. Four methodological approaches were developed, the first three of which resulted in thematic maps of fracture density, drainage density and alteration thickness, using Landsat 8 and airborne geophysical images, Digital Terrain Model (DTM) data and borehole data. Next, four flow classes were defined according to the minimum flow required for the various types of drinking water supply works in Burkina Faso, followed by a study of their distribution on the various thematic maps produced for the definition of the coastlines. Finally, a weighting was made on the basis of coasts and coefficients assigned to each parameter for mapping the hydraulic potential of fissured aquifers. Field data (boreholes, structural measurements and hydrogeological indices) and previous studies were used to validate the mapping. Analysis of the distribution of borehole flow rates on the various thematic maps shows that borehole productivity is optimal for a fracture density of between 1.55 and 1.9 km/km2, a drainage density of between 0.28 and 0.35 km/km2 and an alteration thickness of less than 25 m. Hydraulic potential was mapped using the weighting method, based on the distribution of borehole flow rates on maps of weathering thickness, drainage network density and fracturing density, highlighting three hydrogeological domains: the low-productivity zone, occupying 24.40% of the basin's fissured aquifers, mainly found north of Gaoua, in the south-

central and eastern parts of the basin around Gbomblora; the medium-productivity zone, occupying almost 31.57% of the fractured aquifers, is found mainly in the central-eastern part of the basin between Gaoua and Perigban, to the east of the commune of Gaoua, to the west of Kampti and to the west and north-east of Midebdo; and the good-productivity zone, representing 44, 04% of the basin's fissured aquifers, it is located mainly in the north-western part of the basin, north of Loropéni, east of Kampti, around Perigban and in the south-east, notably north-east of Batié. The high-productivity zones almost overlap with all the Water Production Centers (CPE) identified within the watershed during a hydrogeological study commissioned by COWI in 2019 on the search for high-productivity zones on the crystalline basement. This study constitutes a guide which will guide groundwater research and must be carried out before any land use project.

Keywords

Hydrogeological Potential, Fissured Aquifers, Fracturing Density, Drainage Density, Weathering Thickness, Poni Watershed

1. Introduction

Water resources, particularly groundwater, are the foundation of economic and social development in arid and semi-arid countries (MacDonald et al., 2005). They are essential to the existence of life and the development of ecosystems. According to Carter and Parker (2009), almost half of Africa's population depends on them. In crystalline and crystallophyllous basement zones, the search for groundwater is often highly complex due to the discontinuous nature of the aquifers (Kafando et al., 2016). In these zones, groundwater storage and flow only occur when the rock is fractured and/or altered. Discharge rates from hydraulic structures are generally low. Over the last few decades, studies have shown that in this geological domain, high-flow boreholes are linked to kilometre-long fractures, fracture intersections and highly interconnected fracture networks (Savadogo, 1984; Nakolendoussé, 1991; Savané et al., 1995). Identifying these fractures is therefore one of the mainstays for mapping the hydraulic potential of fissured aquifers. These fractures are generally accompanied by a significant alteration fringe, and are also zones of weakness that can be occupied by watercourses.

In the Poni watershed, the permanent unavailability of surface water and its pollution, as well as the cost of mobilizing it, mean that groundwater is the resource of first choice for supplying drinking water to towns and the country side.

In the crystalline formations, hydrogeologists have invested in the search for high-flow boreholes. Today, some high-flow boreholes have dried up during their operation, as in the case of boreholes (F2 and F7) belonging to the National Office for Water and Sanitation (ONEA) in the town of Gaoua. In addition to dwindling groundwater resources, the uncontrolled occupation of land due to demographic

pressure is limiting groundwater recharge. This is the background to our study, the aim of which is to map the hydraulic potential of fissured aquifers in the Poni watershed. Specifically, the aim is to produce thematic maps of fracture density, drainage network density and alteration thickness.

2. The Poni Watershed

The Poni watershed is located between longitudes 3˚45' and 2˚55' West and latitudes 9˚50' and 10˚36' North in the South-West region of Burkina Faso. It covers an area of 5,453 km^2. It is drained by the Poni river, one of the main tributaries of the Mouhoun.

The climate is Sudanian, with two distinct seasons: a dry season from November to May and a rainy season from June to October, with average annual rainfall of over 900 mm.

The relief is very rugged, with an average altitude of 350 m. It is characterized by a succession of hills and topographical depressions, with a geomorphology dominated by a functional glacis crowned at the southern end by low-lying areas (Figure 1).

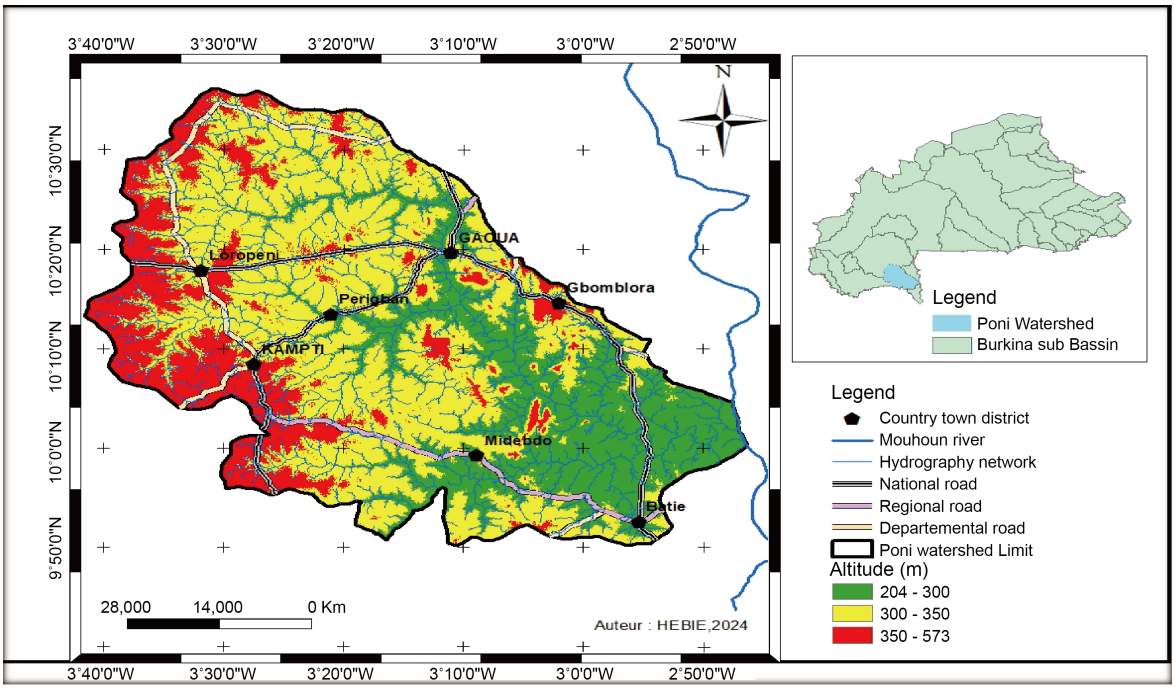

Figure 1. Location map of the Poni watershed (data source: SRTM 2019 image and BNDT 2015).

Lithologically, three series of formations can be distinguished: the volcanic and volcano-sedimentary series, essentially made up of various types of basalt and andesite. These petrographic formations are subsequently intruded by microgranites, microdiorites, rhyolites and dacites. Finally, the sedimentary series of cherts, grauwackes and intercalary graphitic rocks. These three series are successively intruded by granitoids, microgabbros and microdiorites.

In terms of structural geology, recent studies have shown that the geological formations of the Gaoua region were affected by four phases of deformation during the Eburnian orogeny. The structures resulting from these different deformation phases are divided into first-order, second-order, third-order and fourth-order structures. According to (Baratoux et al., 2011), these structures are generally regional, oriented NE-SW and locally NW-SW. There are also shear zones with mylonitic deformation (Ouédraogo & Prost, 1986) and fractures of various orientations intersecting regional structures and shear zones (Ouiya et al., 2020) (**Figure 2**).

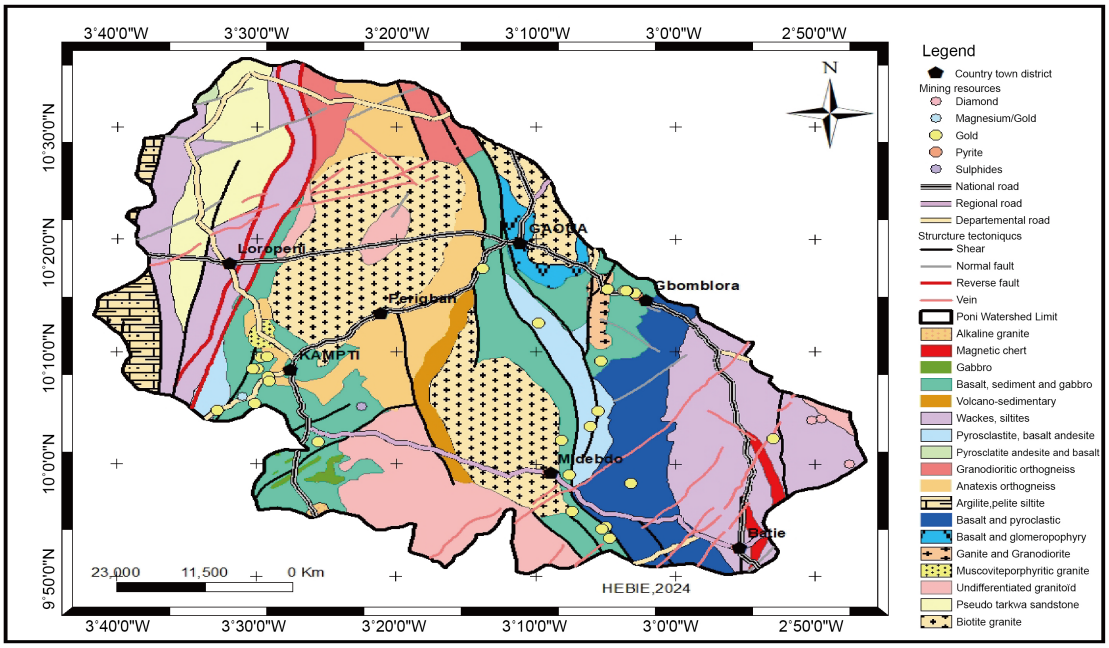

Figure 2. Geological and mining map of the Poni watershed (Data source: BUMIGEB).

Hydrogeologically speaking, groundwater reservoirs in the Poni watershed are divided between alterite aquifers and fissured aquifers. These two types of aquifer are often superimposed and closely linked by drainage (Savadogo, 1984). Alterite aquifers are generally tapped by wells, and their thickness varies between 10 and 20 m in the granite-gneiss formations and between 15 and 40 m in the schists. These aquifers are highly influenced by climatic phenomena.

Fissured aquifers are generally tapped by boreholes at depths ranging from 40 to 120 m. Fissured aquifers play a capacitive role, and are the most sought-after for hydraulic drilling. The productivity of these aquifers is influenced by the lithological facies, the presence or absence of alterites and the hydraulic connectivity of the fractures intersected by the works.

3. Data, Materials and Methodological Approach

1. Data and materials

The database used for this study consists of borehole data, airborne geophysics,

Landsat 8 images and SRTM. In addition to these data, a field trip was carried out to carry out structural measurements on outcrops and to observe the orientation of hydrogeological indices with a view to validating the lineament map.

Landsat data

Landsat 8 OLI images were used for this study. These images are scenes 196 and 195 (path) of row 053, respectively, taken on February 17, 2020 at 10 h 26 mn 37 s and February 24, 2020 at 10h 32 mn 46 s. The shooting period is very important for obtaining good quality images. The various scenes used were downloaded from https://earthexplorer.usgs.gov/ with less than 5% cloud cover, justifying the quality of these images. The DTM data were also downloaded from NASA's USGS (United Stated Geological Survey) website.

Borehole data

A database of four hundred and ninety-six (496) boreholes was compiled as part of this study. This information was collected from regional water authorities, engineering firms and the Department of Study and Information on Water (DEIE).

Airborne geophysical data

Airborne geophysical magnetometry data from the 1999 sysmin project survey covering the Gaoua-Téhini square degree were also used. These data were acquired from the Burkina Mining and Geology Bureau (BUMIGEB).

Field data

Structural measurements were carried out in the field, followed by observation of the orientation of biological indices and hydrophilic trees, in order to confirm or invalidate the mapped structures when interpreting the data. The various measurements were taken using a compass.

Hardware

The data were processed using various software packages. ENVI 4.7 was used to process satellite images. Oasis montaj software was used to process airborne geophysical data. The data from the various processing operations were integrated into ArcGIS 10.5 software to produce fracturing and fracturing density maps. ArcGIS 10.5 was also used to process the DTM data and produce the drainage network density map. RockWork 14 was deployed to produce the directional rosettes.

2. Methodological approach

The methodology used to map the hydrogeological potential of the Poni watershed is based on four approaches:

The first involved processing Landsat 8 images and airborne geophysical data, followed by lineament extraction and validation. The validated lineaments were then used to produce a fracturing density map. The second approach involved generating the hydrographic network from the DTM data to produce the drainage density map. The third approach involved the spatialization of weathering thicknesses from borehole data in the watershed, using the interpolation method. At the level of each approach, a statistical study was carried out on the basis of the flow rates from the boreholes drilled, in order to define the productivity zones for

each thematic map. The fourth approach was to map hydrogeological potential by combining the different productivity zones from the thematic maps.

The first approach

The lineaments resulting from the processing of Landsat 8 images from scenes 195/053 and 196/053 covering the Poni watershed were extracted. Processing involved mosaicking two images (combining the two images) to extract the study area, followed by band ratios (B4/B7, B4/B6, B3/B4, B4/B5). These band ratios reduce the effects of illumination, topography or vegetation, and accentuate the spectral signatures characteristic of certain soils, minerals and rocks.

Following these operations, RGB (Red Green Blue) color compositions, principal component analysis (PCA) and directional filtering were performed. The color compositions highlight contrasts not visible to the naked eye. PCA is a linear transformation that reduces spectral redundancy and extracts the axes of maximum variance in multi-spectral data. Filters play a crucial role in the detection of linear structures. Among filtering methods, Sobel's filters, which use two convolution masks to estimate partial derivatives along two well-defined directions, and those of Yessou and Prewitt, which use well-defined algorithms, have been applied. Image processing using Envi 4.5 software highlighted color contrasts and linear structures that can be assimilated to lithological and structural discontinuities. The various discontinuities, known as lineaments, were extracted manually using ArcGIS 10.5 software.

In addition to Landsat 8 images, airborne geophysical data, in particular aeromagnetic data, were used for lineament mapping.

According to Metelka et al. (2011), aeromagnetic data are highly effective for mapping geological formations and their structures down to a depth of around 300 m. As the raw data were pre-processed by BUMIGEB, processing involved the application of several filters such as Reduction to Poles (RTP)), Vertical Derivative (Vertical Derivative) or vertical gradient Kafando (2020).

RTP aims to bring anomaly signals back to plumb (MacLeod et al., 1993), by transforming an asymmetrical anomaly measured at a given latitude into a simulated symmetrical anomaly at the poles (Baranov, 1957 in Sawadogo, 2017) and the vertical derivative is the vertical gradient of the residual magnetic field, it evaluates the rate of change of the magnetic field of the sources according to depth. The latter filter is very useful for interpreting structural discontinuities. According to Hood, 1965 in Sawadogo (2017), this filter has the advantage of improving the resolution of anomalies close together or superimposed.

Aeromagnetic data were processed using Oasis montaj version 8.4, and lineaments were extracted using ArcGIS 10.5.

Lineaments derived from Landsat 8 image processing and airborne geophysics were verified in the field. Field work consisted of structural measurements on rock outcrops and verification of the directions of hydrogeological and biological indices at Gaoua, Gomblora and Nassara. In addition, the directional rosette from the lineament map was completed and compared with the rosettes from previous studies and the geological map. All anthropogenic linear structures (tracks, roads,

field and forest boundaries and power lines) were eliminated.

The validated lineament map was processed using ArcGIS 10.5 software to determine fracture density. Zones were defined according to fracturing density.

The second approach

Nowadays, many boreholes are drilled through non-recharged fractures, due to low rainfall, low infiltration rates and high evapotranspiration rates (Kafando et al., 2016). In the Sahel region of Burkina Faso, certain works (Armand, 1983 in Kafando, 2014) have shown that high-flow boreholes are generally located on the edge of surface water points. These wetlands are therefore privileged groundwater recharge zones. As a result, the hydrographic network is an important factor to consider when mapping the hydraulic potential of aquifers.

In the present study, the drainage network of the Poni watershed was extracted by processing Digital Terrain Model data on ArcGIS 10.5. As the hydrographic network produced was consistent with that of the topographic map, it was used to produce the drainage network density map. This drainage network density map is used to assess permeability, an important hydrogeological property for groundwater accumulation and recharge.

The third approach

This approach consisted in spatializing the weathering thicknesses of the watershed, based on the weathering thickness data from the boreholes collected. This spatialization was carried out by interpolation using the IDW method, which is a weighting technique of inverse distance. Depending on their nature, alteration thicknesses can act as infiltration water collectors for groundwater recharge and partially control borehole productivity (Nakolendoussé, 1991; Kafando, 2014; Kafando et al., 2016; Sayoba et al., 2018; Kafando, 2020). Fracture zones, shear zones and lithological contact zones are generally characterized by powerful alteration thicknesses (Savadogo, 1984; Nakolendoussé, 1991), the strength of which depends on the type of geological formation. Alteration thicknesses play an important role in groundwater recharge in fissured aquifers, which is why they are taken into account when mapping the watershed's hydraulic potential.

For each of the above approaches, a statistical study was carried out on the basis of data from 496 boreholes. The flow rates of the boreholes collected were divided into four classes: $Q < 0.7\ m^3/h$; $0.7\ m^3 \leq Q < 3\ m^3/h$; $3\ m^3 \leq Q < 5\ m^3/h$ and $Q \geq 5\ m^3/h$, respectively defining zones of very low, low, medium and high productivity. The distribution of borehole flow rates by class was based on the minimum flow rates required for the construction of Human Motricity Pumps (HMPs), Autonomous Water Stations (ASWs) and Simplified Potable Water Supply Systems (SPWSSs).

The fourth approach

This involved mapping the hydraulic potential of fissured aquifers in the Poni watershed using the weighting method. Three zones were defined on each of the three thematic maps, ranked from 1 to 3 on the basis of statistical studies.

Coefficient indices 5, 4 and 3 were assigned respectively to fracture density, drainage network density and alteration thickness, followed by calculation of the

potentiality index according to the formula:

IP = DF*5 + DD*4 + EA*3, with IP: potentiality index; DF: Fracture density; DD: Drainage network density and EA: Alteration thickness. The choice of coefficients 5, 4 and 3 was verified by calculating the consistency index (CR = 0) according to the methodology applied by Saaty (1980) as part of the Analytic Hierarchy Process, which shows that the choice is perfectly consistent, so these coefficients, once normalized give a perfectly consistent comparison matrix.

On the basis of the potentiality indices, three hydrogeological zones or domains have been defined:

- a zone or domain of low hydrogeological productivity, with a potentiality index of less than 17;
- a zone or area of average hydrogeological productivity, corresponding to zones with a productivity index of between 17 and 22;
- and a zone or area of good hydrogeological productivity corresponding to zones with a potentiality index greater than 22.

4. Results

1. Image processing and lineament mapping

Landsat 8 images were processed using the 731 color compositions, Principal Component Analysis of the 567 color composition and NW-SE directional Sobel and Prewitt filtering of the panchromatic band 8, giving conclusive results for detecting lineaments (**Figure 3**). Sobel's 7X7 square matrix filters in the NW-SE direction and Yessou's band 8 and Prewitt's 731 color composition provided interesting results for lineament mapping.

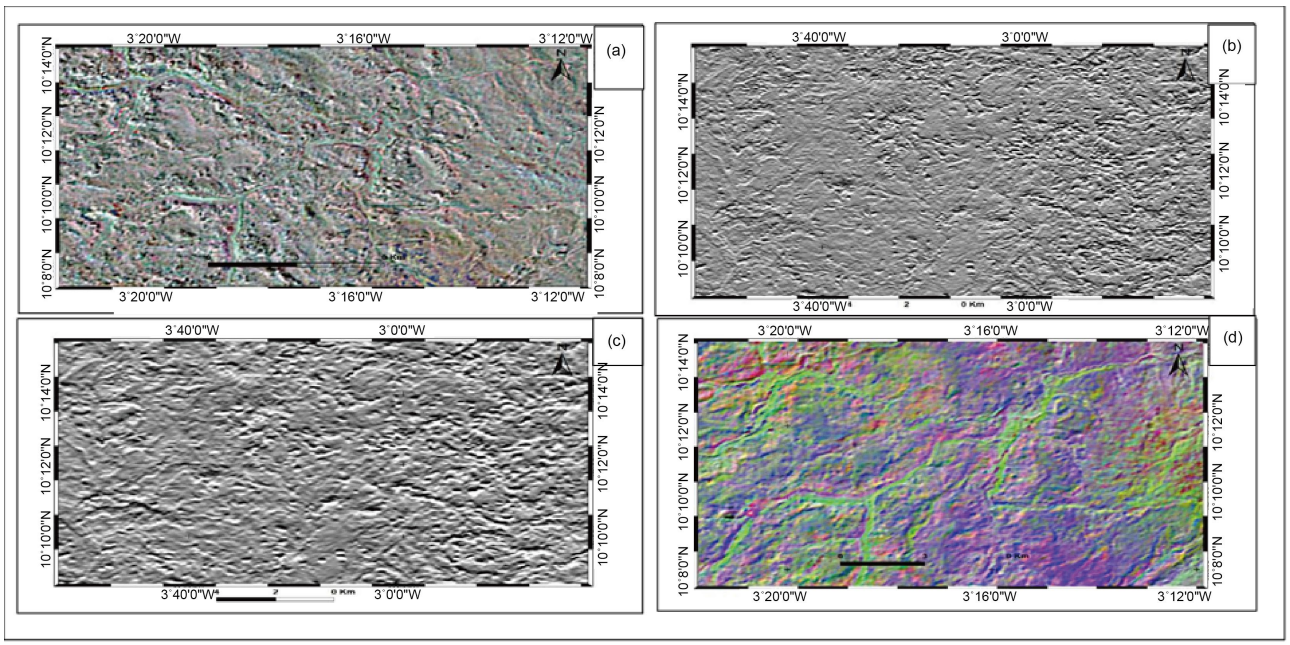

Figure 3. Landsat 8 image processing: (a) prewitt filter for color composition 731, (b) yessou filter applied to band 8, (c) sobel filter with NW-SE orientation for band 8; (d) ACP 1 for color composition 567.

The processing of airborne geophysical images through pole reduction, derivation and total magnetic field, also enabled lineaments to be visualized (Figure 4).

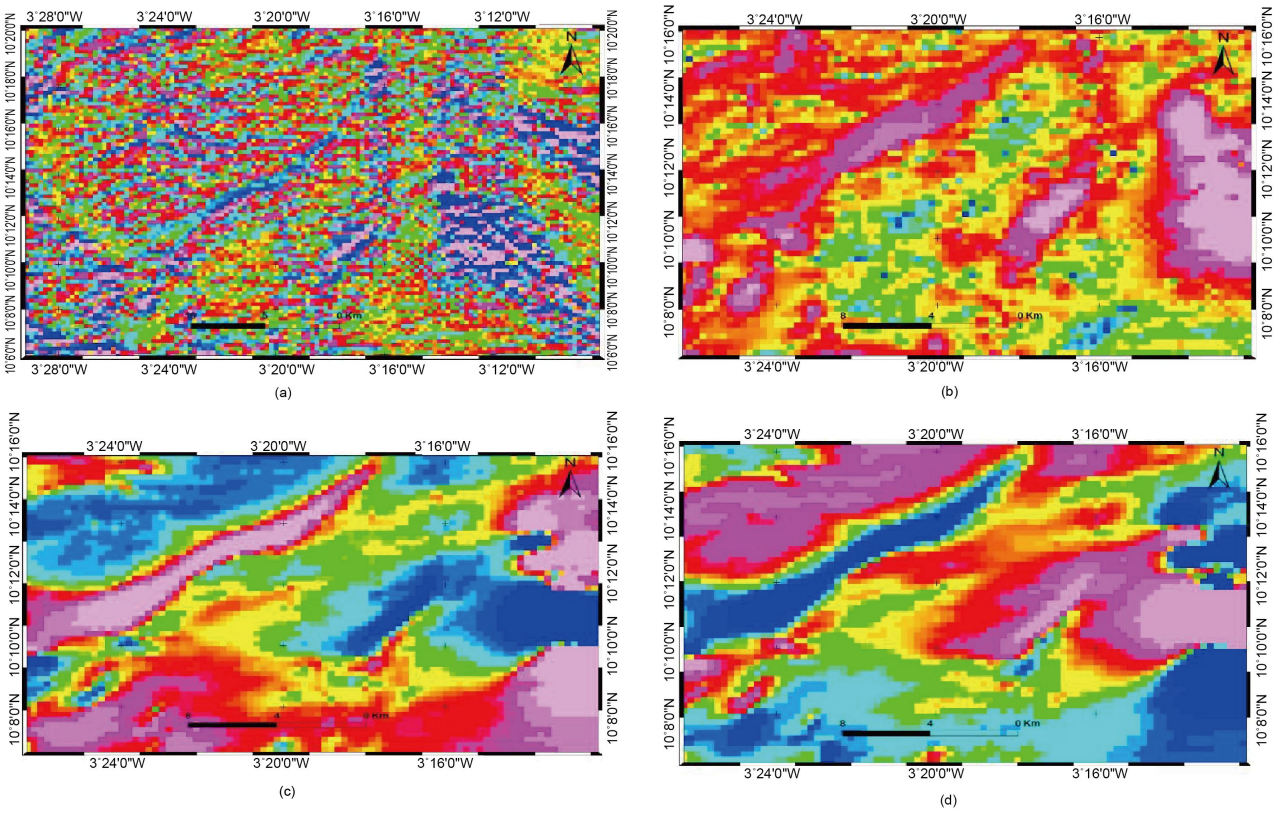

Figure 4. Processing airborne geophysical images: (a) Vertical derivative, (b) Analytical signal, (c) Total magnetic field, (d) reduction to Pole.

2. Lineament validation

To validate the lineaments, the major fractures covering the watershed were first extracted from the 1:1,000,000 Burkina Faso geological and mining maps and the 1:200,000 Gaoua-Téhini square degree maps produced in 2003 as part of the SYSMIN project (Castaing et al., 2003), as well as those produced as part of studies in the area (Baratoux et al., 2011; Ouiya et al., 2020). Superimposing these major fractures extracted from previous lineament study maps shows a very high degree of similarity. In order to validate the lineament map, a field trip was carried out during which the orientation of hydrogeological indices was observed and structural directions measured on rock outcrops. (Figure 5). The structures measured consisted of fractures, veins and schistosities.

Lineaments corresponding to linear structures of anthropogenic origin (tracks, roads, field boundaries, forests and power lines) have been eliminated. Validated lineaments are likely to correspond to fracturing. As a result, 1,242 lineaments were selected for directional studies and fracturing density mapping (Figure 6).

Directional studies show that the dominant lineament directions are predominantly NE-SW and NW-SE, with the N40˚E to N70˚E and N120˚E to N140˚E

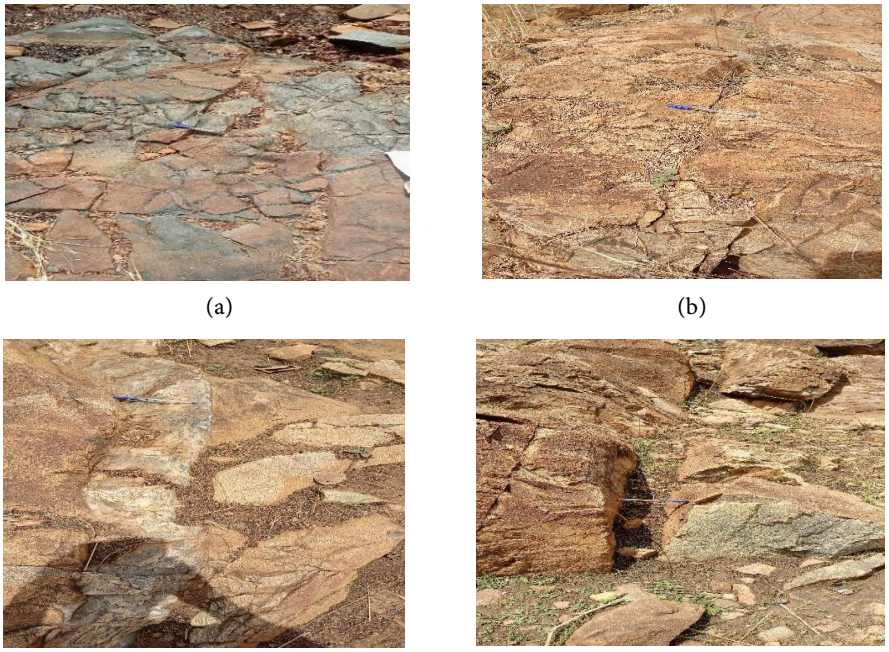

(a) (b)

(c) (d)

Figure 5. Structures measured: (a) fractured greenstone; (b) fractured granite; (c) quartz vein intrusion in a granitic facies followed by fracturing; (d) a mega-fracture on a granitic facies.

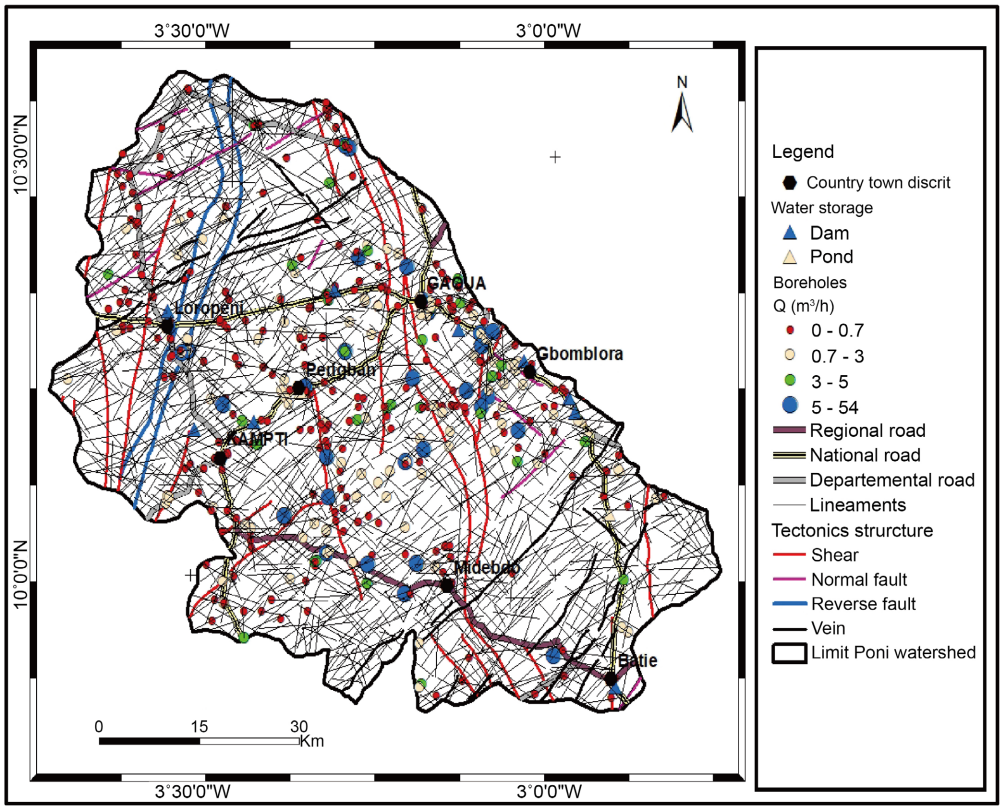

Figure 6. The lineament map (data source: landsat 8 and aeromagnetic images, geological map and BNDT, 2015).

classes emerging (Figure 7(a)). In contrast, the N90˚E to N120˚E class predominates in the structural directions measured on the outcrops (Figure 7(b)), corresponding to the third dominant lineament class mapped. The difference in dominant direction between lineaments and structural measurements could be explained by the restriction of structural measurements around the communes of Gaoua and Gbomblora, due to the inaccessibility of certain sites as a result of security issues, particularly recurrent terrorist attacks, and the scarcity of outcrops in certain parts of the basin.

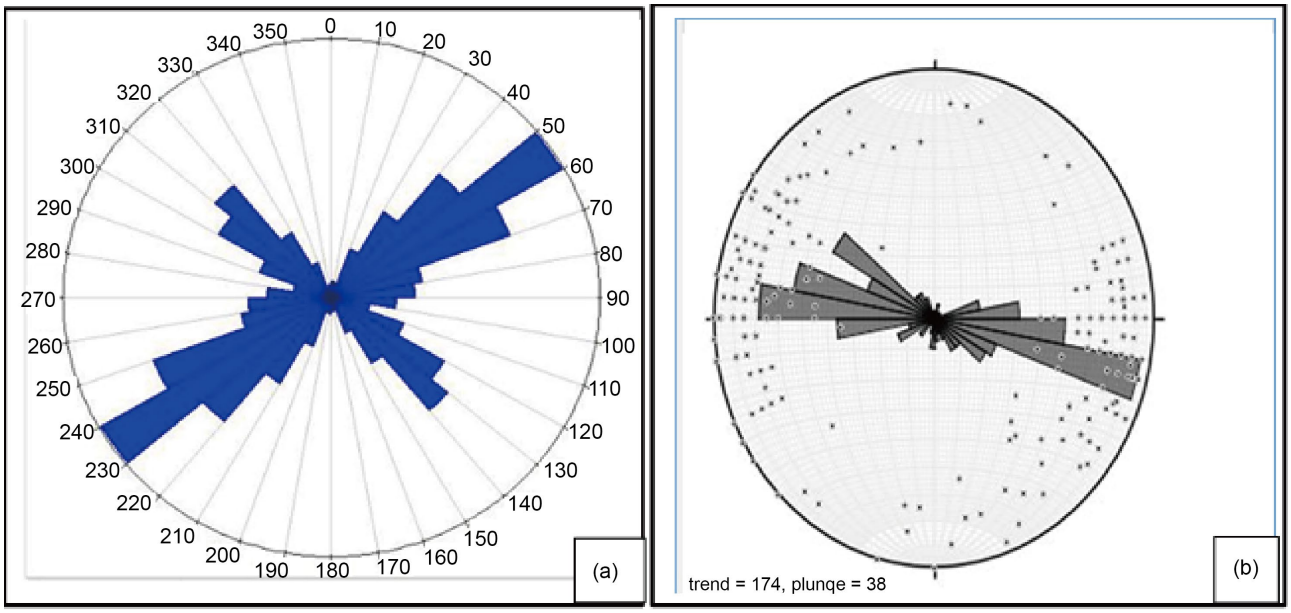

Figure 7. Directional rosettes (a) lineaments (b) structural measurements in the field.

3. Fracture density

The validated lineament map was used to produce the fracture density map. This map, produced on a 10 km × 10 km grid in order to map multi-kilometre structures, shows that fracturing density varies between 0.036 and 2.77 km/km^2 over the watershed. The 10 km × 10 km grid provides a resolution adapted to the regional scale and guarantees a statistically significant density of lineaments in each grid. This grid is widely used in hydrogeological studies in West Africa to link fracturing and drilling productivity (Macdonal et al., 2005; Adiat et al., 2009). On the other hand, the use of a finer mesh does not provide statistical stability, but does identify localized fractured zones. The choice of mesh size depends on the mapping scale.

A statistical study was carried out based on 496 boreholes divided into three fracture density classes (0.036 - 1.55 km/km^2; 1.55 - 1.9 km/km^2 and 1.9 - 2.77 km/km^2) defined according to geometric distribution. In terms of borehole flow rates, four classes were defined ($Q < 0.7$ m^3/h; 0.7 m^3/h $\leq Q < 3$ m^3/h; 3 m^3/h $\leq Q < 5$ m^3/h and $Q \geq 5$ m^3/h) according to productivity. The results of the statistical study are shown in Table 1 below.

Table 1. Distribution of boreholes by fracture density and flow rate.

Flow rate \ Fracture density	0.036 - 1.55 km/km²	1.55 - 1.9 km/km²	1.9 - 2.77 km/km²	Total
Q < 0.7 m³/h	19	52	18	89
0,7 m3/h ≤ Q < 3 m³/h	56	112	56	224
3 m3/h ≤ Q < 5 m³/h	21	34	11	66
Q ≥ 5 m³/h)	35	51	31	117
Total	131	249	116	496
Success rate (Q ≥0.7 m³/h)	22.58%	39.72%	19.76%	82.06%
Rate of drilling (Q ≥ 3 m³/h)	11.29%	17.14%	8.47%	36.90%

Statistical data are analyzed according to the success rate and the rate of boreholes with a flow rate greater than or equal to 3 m³/h. In the Poni watershed, the statistical study shows a success rate of 82.06% in drilling, including 36.90% of boreholes with a flow rate greater than or equal to 3 m³/h.

The distribution of success rates and drillings with a flow rate greater than or equal to 3 m³/h (Q ≥ 3 m³/h) according to fracturing density classes shows that fracturing density between 0.036 and 1.55 km/km² has a success rate of 22.58%, including 11.29% at Q ≥ 3 m³/h; fracturing density between 1.55 and 1.9 km/km² has a success rate of 39.72%, including 17.14% at Q ≥ 3 m³/h; and fracturing density between 1.9 and 2.77 km/km² has a success rate of 19.76%, including 8.47% at Q ≥ 3 m³/h.

Borehole productivity is thus defined on the basis of the success rate, i.e. borehole flow rate greater than or equal to 0.7 m³/h, and the rate of obtaining a flow rate Q ≥ 3 m³/h. As a result, the zone with a fracture density of between 0.036 and 1.55 km/km² is classified as a medium-productivity zone; the zone with a fracture density of between 1.55 and 1.9 km/km², a high-productivity zone; and the zone with a higher fracture density fluctuating between 1.9 and 2.77 km/km², a low-productivity zone (**Figure 8**).

4. Drainage density

The drainage density map of the Poni watershed shows that drainage density ranges from 0.014 to 0.49 km/km².

A statistical study was carried out on the basis of 496 boreholes divided into three drainage density classes (0.014 -0.28 km/km²; 0.28 - 0.35 km/km² and 0.35 - 0.49 km/km²) defined according to geometric distribution. In terms of borehole flow rates, four classes were also defined (Q < 0.7 m³/h; 0.7 m³/h ≤ Q < 3 m³/h; 3 m³/h ≤ Q < 5 m³/h and Q ≥ 5 m³/h) according to productivity. The results of the statistical study are recorded in **Table 2** below.

The statistical study shows that 25.40% of the success rate is achieved, including 9.27% with Q ≥ 3 m³/h for drainage density below 0.28 km/km²; 40.72% of the success rate, including 21.17% with Q ≥ 3 m³/h for drainage density between 0.28

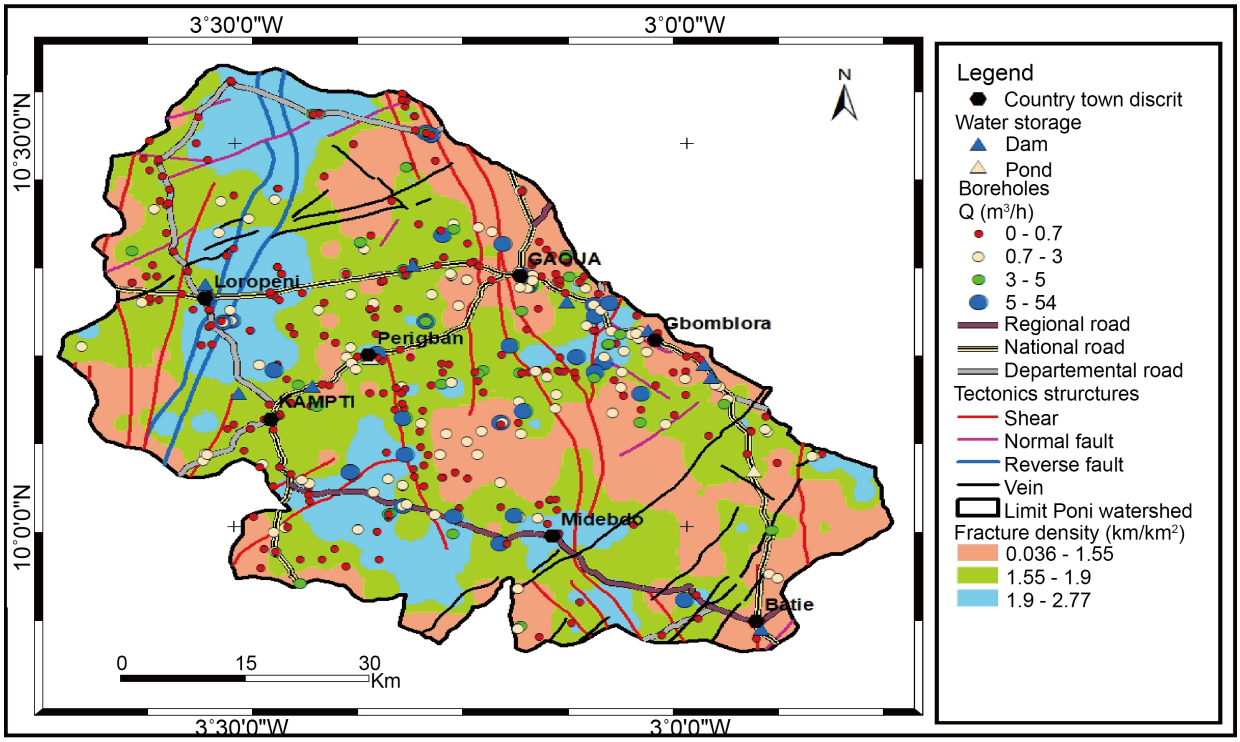

Figure 8. The fracturing density map (data source: landsat 8 and aeromagnetic images, geological map and BNDT, 2015).

Table 2. Distribution of boreholes according to drainage density and flow rates.

Drainage density / flow rates	0.014 - 0.28 km/km²	0.28 - 0.35 km/km²	0.35 - 0.49 km/km²	Total
$Q < 0.7$ m³/h	22	47	20	89
0.7 m³/h $\leq Q < 3$ m³/h	80	97	47	224
3 m³/h $\leq Q < 5$ m³/h	25	29	12	66
$Q \geq 5$ m³/h	21	76	20	117
Total	148	249	99	496
Success rate ($Q \geq 0.7$ m³/h)	25.40%	40.72%	15.93%	82.06%
Rate of drilling ($Q \geq 3$ m³/h)	9.27%	21.17%	6.45%	36.90%

and 0.35 km/km². The drainage density between 0.35 and 0.49 km/km² has a success rate of 15.93%, including 6.45% with $Q \geq 3$ m³/h. This method shows that productive boreholes are located in areas with a drainage density of between 0.28 and 0.35 km/km².

Following the statistical study, three productivity zones were defined on the basis of the success rate and that of obtaining a $Q \geq 3$ m³/h. The medium-productivity zone has a drainage density of less than 0.28 km/km²; the high-productivity zone has a drainage density of between 0.28 and 0.35 km/km²; the low-productivity zone has a drainage density of over 0.35 km/km² (**Figure 9**).

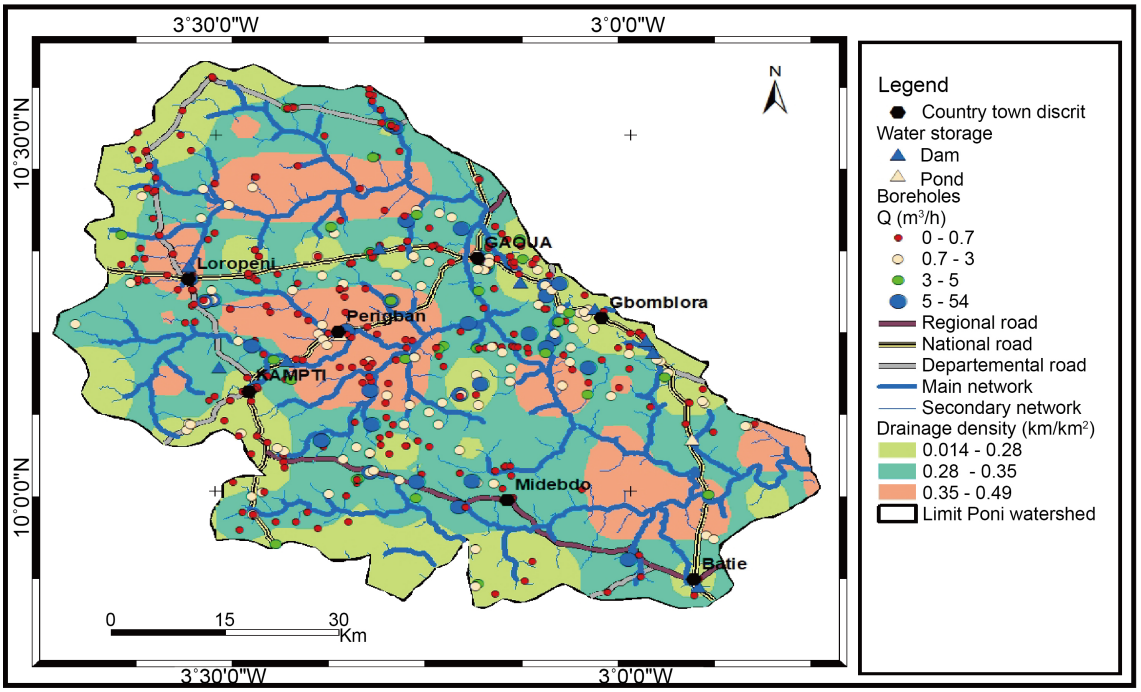

Figure 9. Drainage network density (data source: DTM, 2019 and BNDT, 2015).

5. Weathering thickness

The weathering thickness map of the Poni watershed shows that weathering thicknesses range from 5 to 74 m.

A statistical study was carried out based on 496 boreholes divided into three classes according to weathering thickness (5 - 25 m; 25 m – 35 m; and 35 - 74) defined according to the geometric distribution in the basin. In terms of borehole flow rates, four classes were also defined ($Q < 0.7$ m³/h; 0.7 m³/h $\leq Q < 3$ m³/h; 3 m³/h $\leq Q < 5$ m³/h and $Q \geq 5$ m³/h) according to productivity. The results of the statistical study are shown in Table 3 below.

Table 3. Borehole distribution by weathering thickness and flow rate.

Alteration thicknesses / Flow rate	5 - 25 m	25 -- 35 m	40 - 74 m	Total
$Q < 0.7$ m³/h	41	24	24	89
0.7 m³/h $\leq Q < 3$ m³/h	94	72	58	224
3 m³/h $\leq Q < 5$ m³/h	25	22	19	66
$Q \geq 5$ m³/h	52	33	32	117
Total	212	151	133	496
Success rate ($Q \geq 0.7$ m³/h)	34.48%	25.60%	21.98%	82.06%
Rate of drilling ($Q \geq 3$ m³/h)	15.52%	11.09%	10.28%	36.90%

The statistical study shows that boreholes with alteration thicknesses between

5 and 25 m have a success rate of 34.48%, including 15.52% with a Q ≥ 3 m³/h; a success rate of 25.60%, including 11.09% with a Q ≥ 3 m³/h for boreholes with alteration thicknesses between 25 and 35 m. Boreholes with alteration thicknesses between 35 and 74 m show a success rate of 21.98% including 10.28% at a Q ≥ 3 m³/h (Figure 10).

Based on the statistical study, three zones were defined on the basis of the success rate and the rate of boreholes with a Q ≥ 3 m³/h. Thus, a high-productivity zone with alteration thicknesses below 25 m, a medium-productivity zone with alteration thicknesses between 25 and 35 m, and a low-productivity zone with alteration thicknesses above 35 m.

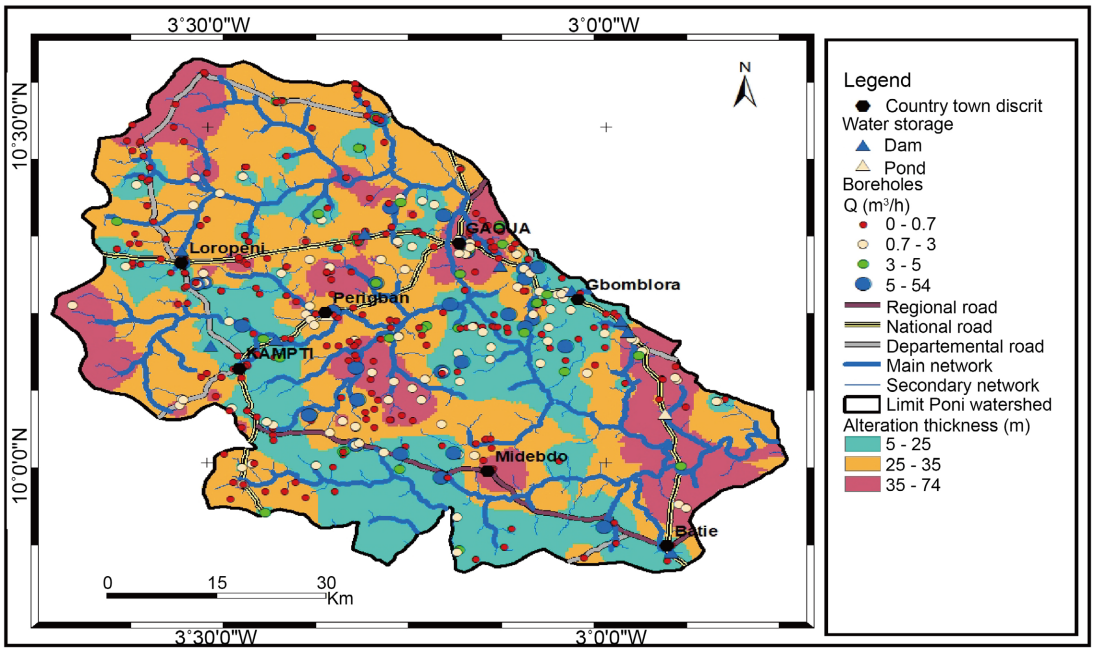

Figure 10. The weathering thickness map (data source: borehole data, geological map and BNDT, 2015).

6. Hydraulic potential of fractured aquifers in the Poni watershed

The hydraulic potential of the basin's fissured aquifers was mapped using a weighting method based on the distribution of borehole flow rates collected on maps of fracturing density, drainage density and alteration thickness. This mapping enabled us to define three hydrogeological domains or zones of hydraulic potential:

- The low-productivity zone occupies 1,330.45 km² of the basin's surface area, i.e. 24.40% of the basin's fractured aquifers. This zone is unevenly distributed throughout the basin, but is mainly represented to the north of Gaoua, in the south-central part of the basin and to the east around Gbomblora.
- The medium productivity zone occupies almost 31.57% of fissured aquifers. It is mainly found in the central-eastern part of the basin between Gaoua and Perigban, to the east of the Gaoua commune, to the west of Kampti and to the west and north-east of Midebdo.

- The high-productivity zone accounts for 44.04% of the basin's fissured aquifers. It is strongly represented in the north-western part of the basin, north of Loropéni, east of Kampti, around Perigban and in the south-eastern part, notably north-east of Batié. This zone almost overlaps with all the Water Production Centers (CPE) identified within the watershed during a hydrogeological study commissioned by COWI in 2019 on the search for high-productivity zones on the crystalline basement (Figure 11).

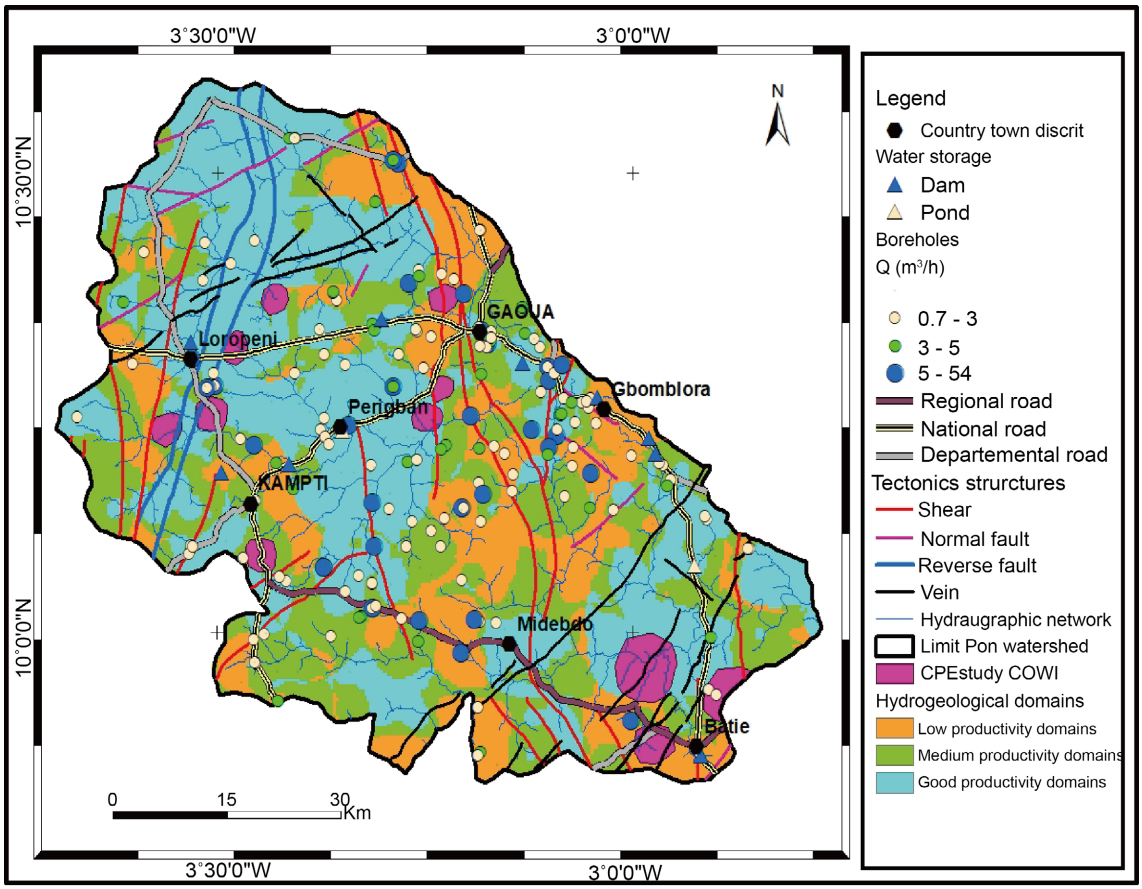

Figure 11. Hydraulic potential of fissured aquifers in the Poni watershed.

5. Discussion

The fracture density map shows that drilling productivity is linked to fracture density. To this end, there are fracturing density thresholds below and above which drilling productivity is lower. Low fracture density (0.036 to 1.55 km/km^2) could be explained by the short length or interconnection of lineaments, which does not allow groundwater to accumulate. Drilling productivity is optimal when fracture density is between 1.55 and 1.9 km/km^2. The drop in productivity in the zone of very high fracturing density (1.9 to 2.77 km/km^2) could be explained by the clayey nature of the alterites in these highly altered zones. The clayey nature of the alterites does not allow groundwater to accumulate and recharge. In West Africa, several studies (Savadogo, 1984; Nakolendoussé, 1991) carried out in the

crystalline and crystallophyllous basement show that high-flow boreholes are located close to interconnected fracture networks, kilometric fractures and fracture intersections.

The drainage density map of the Poni watershed shows that low drainage density (0.014 to 0.28 km/km^2) and high drainage density (0.35 to 0.49 km/km^2) do not allow groundwater to accumulate. In hydrogeology, it is well known that the drainage network favours runoff and limits infiltration. However, in the Poni watershed, there are drainage density thresholds below and above which groundwater accumulation and recharge are limited. Drainage density of between 0.28 and 0.35 km/km^2 occupies an area of high drilling productivity in the basin. This may be explained by the fact that the drainage density between 0.28 and 0.35 km/km2 corresponds to structural faults that allow aquifers to be recharged. Research carried out in the crystalline basement environment (Edet et al., 1998) has shown that there is a correlation between drainage density and the permeability of geological formations. The work of Faillat (1986) also showed a strong correlation between the drainage network and regional faults. The drainage network has been used as a recharge factor for fractured aquifers by many authors (Sener et al., 2005; Shaban et al., 2006; Yeh et al., 2009; Krishnamurthy et al., 1996).

The weathering thickness map of the Poni watershed shows that the majority of high-flow boreholes have weathering thicknesses of less than 25m. These alteration thicknesses enable infiltration water to be collected for groundwater recharge. Borehole productivity decreases when alteration thickness exceeds 25 m. Previous studies have shown that weathering thicknesses act as collectors and partially control borehole productivity (Nakolendoussé, 1991; Kafando, 2014).

Mapping of the hydraulic potential of fissured aquifers in the Poni watershed, using the weighting method based on the distribution of borehole flow rates according to fracture density, alteration thickness and drainage density, has highlighted three hydrogeological domains: the low-productivity zone occupying 1,330.45 km^2 of the watershed surface area, i.e. 24.40% of the fissured aquifers in the watershed. This zone is unevenly distributed throughout the basin, but is mainly found north of Gaoua, in the south-central part of the basin and in the eastern part around Gbomblora; the medium-productivity zone occupies almost 31.57% of fissured aquifers. It is mainly found in the central-eastern part of the basin between Gaoua and Perigban, east of the commune of Gaoua, west of Kampti and west and north-east of Midebdo. The high-productivity zone accounts for 44.04% of the basin's fissured aquifers, and is strongly represented in the north-western part of the basin, north of Loropéni, east of Kampti, around Perigban and in the south-eastern part, notably north-east of Batié. This zone contains almost all the Water Production Centers (CPE) identified within the watershed during a hydrogeological study commissioned by COWI in 2019 on the search for high-productivity zones on the crystalline basement.

Zones with high hydraulic potential for fissured aquifers represent areas of the basin where fracturing and infiltration rates could be significant.

According to some studies (Nakolendoussé et al., 1993; Jourda, 2005; Jourda et al., 2006) carried out in the crystalline basement, the most productive drilling sites should be superimposed on zones with high hydraulic potential, high lineament density, high alteration thickness and high node density.

The advantage of this approach is that it mobilizes low costs and saves time for studies covering vast areas. However, the main difficulty lies in defining the class boundaries of the various maps of alteration density and thickness, and digitizing the exact class boundaries to produce the hydraulic potentiality map of fissured aquifers. It should be emphasized that the boundaries of the various classes defined must be perceived as transition zones between the different classes and not as tangible barriers.

Validation of the hydraulic potential map of fissured aquifers in the Poni watershed was achieved by superimposing the results of the hydrogeological study commissioned by the Danish cooperation COWI in 2019. The purpose of this study was to map areas of high hydrogeological potential in the crystalline basement of the Boucle du Mouhoun, Cascades, Hauts-Bassins and South-West regions. As a result of this study, high-potential zones were identified for use as Water Production Centers (CPE). Most of the WPCs in the Poni watershed are located in areas of high mapped productivity.

However, it should be noted that in the crystalline basement, the productivity of boreholes is linked to the presence of fractures, their length and their opening. In the high-potential zone, negative and low-flow boreholes may be encountered, but the probability of this happening remains low. For this reason, the high-potential zone should be targeted for ground geophysical investigations for any project involving the construction of high-flow boreholes or a water production center.

6. Conclusion

Mapping the hydraulic potential of fissured aquifers in the Poni watershed using the weighting method, based on the distribution of borehole flow rates on maps of fracture density, drainage density and alteration thickness, has revealed three hydrogeological domains: the low-productivity zone occupying 24.40% of the basin's fractured aquifers; the medium-productivity zone representing the major 31.57% of the catchment area and the high-productivity zone occupying 44.04% of the fractured aquifers, this zone overlaps with most in high-productivity zones mapped to serve Water Production Centers as part of a Danish COWI cooperation project in 2019.

The distribution of borehole flow rates on the various thematic maps used to map the hydraulic potential of fissured aquifers in the Poni watershed shows that there is a range of values on each map for which the productivity and/or recharge of the structures is optimal. Productivity and/or recharge of catchment structures in fissured aquifers in the Poni watershed are optimal for drainage density of be-

tween 0.28 and 0.35 km/km^2; fracturing density of between 1.55 and 1.9 km/km^2; and alteration thicknesses of less than 25 m. This methodology is highly pragmatic for the study of large watersheds in sub-Saharan Africa, characterized by the scarcity or absence of hydrogeological data.

Looking ahead, we plan to undertake ground geophysical investigations followed by boreholes to refine the hydraulic potential map of the fissured aquifers in the watershed.

Conflicts of Interest

The authors declare no conflicts of interest regarding the publication of this paper.

References

Adiat, K. A. N., Olayanju, G. M., Omosuyi, G. O., & Ako, B. D., 2009. Electromagnetic Profiling and Electrical Resistivity Soundings in Groundwater Investigation of a Typical Basement Complex—A Case Study of Oda Town Southwestern Nigeria. *Ozean Journal of Applied Sciences, 2,* 333-359.

Baranov, V. (1957). A New Method for Interpretation of Aeromagnetic Maps: Pseudo-Gravimetric Anomalies. *Geophysics, 22,* 359-382. https://doi.org/10.1190/1.1438369

Baratoux, L., Metelka, V., Naba, S., Jessell, M. W., Grégoire, M., & Ganne, J. (2011). Juvenile Paleoproterozoic Crust Evolution during the Eburnean Orogeny (~2.2-2.0 Ga), Western Burkina Faso. *Precambrian Research, 191,* 18-45. https://doi.org/10.1016/j.precamres.2011.08.010

Carter, R. C., & Parker, A. (2009). Climate Change, Population Trends and Groundwater in Africa. *Hydrological Sciences Journal, 54,* 676-689. https://doi.org/10.1623/hysj.54.4.676

Castaing, C., Bila, M., Milési, J.-P., Thiéblemont, D., Le Metour, J., Egal, E. et al. (2003). *Explanatory Note for the 1:1,000,000 Geological and Mining Map of Burkina Faso* (3rd Ed., pp. 1-148). BRGM, Orléans, and BUMIGEB, Ouagadougou.

Edet, A. E., Okereke, C. S., Teme, S. C., & Esu, E. O. (1998). Application of Remote-Sensing Data to Groundwater Exploration: A Case Study of the Cross River State, Southeastern Nigeria. *Hydrogeology Journal, 6,* 394-404. https://doi.org/10.1007/s100400050162

Faillat, J. P. (1986). *Aquifèrs fissures en zone tropical humide: Structure, hydrodynamisme et hydrochimie en Afrique de l'ouest* (534 p.). Thèse de doctorat, Université de Montpellier.

Jourda, J. P. (2005). *Methodology for the Application of Remote Sensing Techniques and the Concept of Spatial Hydrotechnics: The Case of Test Areas in Côte d'Ivoire* (430 p.). State Thesis, Univ. Cocody, Côte d'Ivoire.

Jourda, J. P. R., Saley, M. B., Djagoua, E. V., Kouamé, K. J., Biemi, J., & Razack, M. (2006). Use of Landsat ETM+ Data and GIS for the Assessment of Groundwater Potential in the Precambrian Fissured Environment of the Korhogo Region (Northern Ivory Coast): Multi-Criteria Analysis Approach and Validation Test. *Remote Sensing, 4,* 339-357.

Kafando, S. (2014). *Improved Knowledge of Groundwater Resources in Burkina Faso: Case of the Hydrogeological Map of the Sahel Region* (102 p.). Master's Thesis II, University of Ouagadougou.

Kafando, S. (2020). *Hydrogeological Characterization and Groundwater Potential in the Middle of the Crystalline Basement: Case of the Ouagadougou Sheet. Geology-Geophysics-Remote Sensing* (234 p). Thesis, Joseph KI-ZERBO University.

Kafando, S., Nakolendoussé, S., Nikiema, J., Koussoubé, I., Yaméogo, S., Compaoré, Y., & Millogo, C. (2016). Geomorphology and Productivity of Aquifers in a Crystalline Basement Environment: Case of the Central Region of Burkina Faso. *Annal of Ouaga University Series C, 12,* 45-47.

Krishnamurthy, J., Venkatesa Kumar, N., Jayaraman, V., & Manivel, M. (1996). An Approach to Demarcate Ground Water Potential Zones through Remote Sensing and a Geographical Information System. *International Journal of Remote Sensing, 17,* 1867-1884. https://doi.org/10.1080/01431169608948744

Macdonald, S. E., Burton, P. J., Chen, J., Brosofske, K. D., Saunders, S. C., Esseen, P. A. et al. (2005). Edge Influence on Forest Structure and Composition in Fragmented Landscapes. *Conservation Biology, 19,* 768-782. https://doi.org/10.1111/j.1523-1739.2005.00045.x

MacLeod, I. N., Jones, K., & Dai, T. F. (1993). 3-D Analytic Signal in the Interpretation of Total Magnetic Field Data at Low Magnetic Latitudes. *Exploration Geophysics, 24,* 679-687. https://doi.org/10.1071/eg993679

Metelka, V., Baratoux, L., Naba, S., & Jessell, M. W. (2011). A Geophysically Constrained Litho-Structural Analysis of the Eburnean Greenstone Belts and Associated Granitoid Domains, Burkina Faso, West Africa. *Precambrian Research, 190,* 48-69. https://doi.org/10.1016/j.precamres.2011.08.002

Nakolendoussé, S. (1991). *Methods for Evaluating the Productivity of Aquifer Sites in Burkina Faso. Geology-Geophysics-Remote Sensing* (256 p.). UJF Thesis.

Nakolendoussé, S., Savadogo, A. N., & Rouleau, S. (1993). *Factors in the Productivity of the Aquifers of the Crystalline Basement of Burkina Faso: The Example of Pobé Mengao* (pp. 95-107).

Ouédraogo, M. F., & Prost, A. E. (1986). Relationships between Schistosity and Folding within the Birimian Yako-Batie Greenstone Belt (Burkina Faso). *Comptes Rendus de l'Academie des Sciences 303,* 1713-1718.

Ouiya, P., Naba, S., Ilboudo, H., Sawadogo, S., Yameogo, A. O. (2020). Identification of Main and Related Structures Controlling Mineralization in the Nassara Gold District in the Southwest of Burkina Faso (West Africa). *Journal of Sciences, 1,* 1-21.

Saaty, T. L. (1980). *The Analytic Hierarchy Process: Planning, Priority Setting, Resource Allocation*. McGraw-Hill.

Savadogo, A. N. (1984). *Geology and Hydrogeology of the Crystalline Basement of Upper Volta. Regional Studies of the Sissili Watershed*. Doctoral Thesis, Scientific and Medical University of Grenoble.

Savané, I., Bénié, G. B., Gwyn, Q. H. J., & Biémi, J. (1995). Application of Remote Sensing to the Search for Groundwater in a Crystalline Environment: Case of Odienné, Ivory Coast. In AUPELF-UREF, *Remote Sensing and Water Resources, 5th Scientific Day of Tunis* (pp. 111-120), University of Quebec Press.

Sawadogo, S. (2017). *The Granitic Plutons of the Djibo Belt in Northern Burkina Faso (West Africa): Emplacement Mechanisms and Implications in the Geodynamic Evolution of the Belt* (304 p.). PhD Thesis, Université Ouaga I-Pr KI-Zerbo.

Sayoba, K., Samuel, N., & Julien, N. (2018). Modeling of the Alteration Wedge in a Crystalline Basement Environment: Case Study of Burkina Faso Central Regions. *Sustainability in Environment, 3,* 83-103. https://doi.org/10.22158/se.v3n1p83

Sener, E., Davraz, A., & Ozcelik, M. (2005). An Integration of GIS and Remote Sensing in Groundwater Investigations: A Case Study in Burdur, Turkey. *Hydrogeology Journal, 13,* 826-834. https://doi.org/10.1007/s10040-004-0378-5

Shaban, A., Khawlie, M., & Abdallah, C. (2006). Use of Remote Sensing and GIS to Determine Recharge Potential Zones: The Case of Occidental Lebanon. *Hydrogeology Journal, 14,* 433-443. https://doi.org/10.1007/s10040-005-0437-6

Yeh, H., Lee, C., Hsu, K., & Chang, P. (2009). GIS for the Assessment of the Groundwater Recharge Potential Zone. *Environmental Geology, 58,* 185-195. https://doi.org/10.1007/s00254-008-1504-9